EUROPHYSICS LETTERS 15 June 2002

Europhys. Lett., **58** (6), pp. 912–918 (2002)

Novel core-shell structure for colloids made of neutral/polyelectrolyte diblock copolymers and oppositely charged surfactants

P. Hervé[1], M. Destarac[2], J.-F. Berret[1](*), J. Lal[3], J. Oberdisse[4] and I. Grillo[5]

[1] *Complex Fluids Laboratory, CNRS-Cranbury Research Center Rhodia Inc. 259 Prospect Plains Road CN 7500, Cranbury, NJ 08512, USA*
[2] *Rhodia, Centre de Recherches d'Aubervilliers - 52 rue de la Haie Coq F-93308 Aubervilliers Cedex, France*
[3] *IPNS Division, Argonne National Labs 9700 South Cass Avenue, Argonne IL 60439, USA*
[4] *Laboratoire Léon-Brillouin, CEA Saclay - F-91191 Gif-sur-Yvette, France*
[5] *Institute Laue-Langevin - BP 156, F-38042 Grenoble cedex 9, France*

(received 21 November 2001; accepted in final form 20 March 2002)

PACS. 82.70.Dd – Colloids.

Abstract. – Using neutron and light scattering experiments, we show that neutral/polyelectrolyte diblock copolymers and oppositely charged surfactants in dilute aqueous solutions associate into colloidal aggregates which have an original core-shell microstructure. We have found that the core is constituted of densely packed surfactant micelles, most likely connected between them by the polyelectrolyte blocks. The outer part of the colloid is a corona and is made of the neutral chains. We suggest that the mechanism of formation of these colloids is identical to that of the associative transition reported in homopolyelectrolyte/surfactant solutions. However, here, the macroscopic phase separation is hindered by the presence of the neutral chains.

When polyelectrolytes and oppositely charged surfactants are mixed in solution, a phase separation generally occurs. While the upper phase is transparent and contains essentially the solvent, the lower phase appears as a precipitate, or eventually as a viscous liquid and contains the majority of the polyelectrolyte and surfactant species [1]. Known for more than 50 years, this phase separation was first discovered in biological systems and used, *e.g.*, as a purification process for proteins. In recent years, the structure of the concentrated phase has attracted much attention. Using scattering experiments [2–7], it has been shown that the precipitates present a long-range order reminiscent of the structures classically found in surfactant/water concentrated phases. Cubic, hexagonal and lamellar symmetries have been observed so far, although the total amount of surfactant and polymer can be as low as some

(*) E-mail: jeanfrancois.berret@us.rhodia.com

© EDP Sciences

weight percents. Very recently, Hansson has suggested that the mechanism of the transition is the associative and cooperative binding of the polyions with the micellar aggregates [8].

Using a neutral/polyelectrolyte diblock copolymer instead of a homopolyelectrolyte, the transition discussed above ceases to occur. In the same range of concentrations and surfactant-to-polymer ratios, the solutions are homogeneous and transparent. As reported recently [9], in neutral/polyelectrolyte diblocks with oppositely charged surfactants, the phase separation is replaced by the formation of finite-size colloids made of both surfactant and copolymers. These colloids have attracted much interest because of their high potential use in pharmaceutics, as drug and gene delivery systems. Termed "block ionomers complexes" [9], these colloids are of spherical symmetry, with typical sizes of the order 1000 Å. It has been suggested that the colloids form spontaneously and have core-shell structure [9]. Except in one case where unilamellar vesicles were recognized, to our knowledge, the exact microstructure of these colloids as well as the mechanism yielding to their formation have not been established.

We have undertaken a systematic study of the phase behaviors of poly(sodium acrylate)-b-poly(acrylamide) block copolymers (noted thereafter PANa-PAM) with cationic surfactants. The properties mentioned above, the phase separation for the homopolymers and the formation of colloids for the diblocks have been confirmed. In this letter, we focus on the microstructure of the colloids resulting from the association between PANa-PAM diblocks with dodecyltrimethylammonium bromide (DTAB). Light scattering and small-angle neutron scattering experiments have been used to this aim, and these techniques reveal a novel core-shell microstructure. For these mixed diblock copolymer-surfactant colloids, we have found that the core is constituted of densely packed surfactant micelles connected between them by polyelectrolyte blocks. The outer part of the colloid is a corona and it is made of the neutral blocks. These results suggest that the mechanism of formation is the associative binding between the charged species, as for homopolyelectrolytes, but the presence of the neutral blocks prevents the macrocroscopic phase separation from occurring.

PANa-PAM copolymers were synthesized by controlled radical polymerization in solution. The synthesis is based on the Madix technology which consists in a novel-transfer-agent–mediated reaction developed by Rhodia [10]. Here we report on a diblock with average molecular weight 35000 g/mol (polydispersity index 1.6), made of 70 monomers of acrylic acid ($M_{\mathrm{w}} = 5000$ g/mol) and 420 monomers of acrylamide monomers ($M_{\mathrm{w}} = 30000$ g/mol). In solution, the acrylic acid monomers were ionized by addition of an equivalent amount of sodium hydroxide up to pH 7-8. The PANa-PAM/DTAB samples were obtained by mixing stock solutions of copolymer and of surfactant prepared at the same weight concentration c. A phase diagram has been established, that we expressed in terms of the concentration c, and of a parameter Z. Z is the ratio between the surfactant and acrylate monomer contents ($Z = 0$ and $Z = \infty$ denote, respectively, pure polymer and pure surfactant solutions). For all concentrations investigated, covering the range 0.01 wt% to 20 wt%, there exists a critical value of Z, noted Z_{C}, above which the surfactant/diblock colloids are formed. Z_{C} depends only slightly on the total concentration and is found ~ 0.2–0.5.

Dynamical light scattering was performed on a Brookhaven spectrometer (BI-9000AT autocorrelator) for sample characterization and for the measurements of the diffusion constant $D(c)$. From the extrapolation of $D(c)$ to infinite dilution, the hydrodynamic radius of the colloids was determined through the Stokes-Einstein relation, $R_{\mathrm{H}} = k_{\mathrm{B}}T/6\pi\eta_{\mathrm{S}}D(c \to 0)$, where k_{B} is the Boltzmann constant, T the temperature ($T = 298$ K) and η_{S} the solvent viscosity. Small-angle neutron scattering (SANS) was performed at three different neutron facilities, at Argonne, at the Laboratoire Léon Brillouin and at the Institute Laue-Langevin. All runs were consistent with each other. In this letter, only the data obtained on the D22 beam line of the Institute Laue-Langevin are shown and discussed. Solutions at concentra-

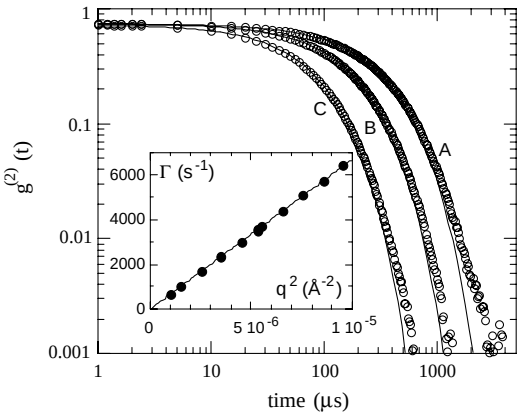

Fig. 1

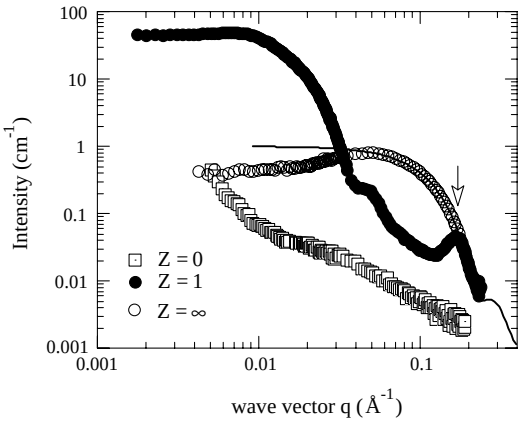

Fig. 2

Fig. 1 – Autocorrelation functions of the intensity scattered by a solution of neutral-polyelectrolyte copolymer (PANa-PAM) and oppositely charged surfactant (DTAB). The total weight concentration is $c = 0.1\%$ and the ratio between surfactant and acrylate monomer molar concentrations is $Z = 1$. The data correspond to experiments performed at wave vectors $q = 1.6$ (A), 2.1 (B) and 3.0×10^{-3} Å^{-1} (C). Continuous lines are single exponential functions with decay rate 2Γ. Inset: evidence of the quadratic dependence of Γ *vs.* wave vector.

Fig. 2 – Neutron scattering intensities obtained on $c = 1\%$ PANa-PAM/DTAB aqueous solutions for $Z = 0$ (pure copolymer), $Z = 1$ and $Z = \infty$ (pure surfactant). The arrow indicates the structure factor peak at $q_0 = 0.16$ Å^{-1}. The continuous line represents the form factor of polydisperse and homogeneous DTAB micelles of average radius $\bar{R} = 20.7$ Å.

tions $c = 0.25\%$–20% and surfactant-to-monomer ratios $Z = 0$–∞ were prepared using D_2O for contrast reasons and investigated by SANS. In the present letter, we focus on dilute solutions at $c = 0.25\%$, 0.5% and 1% and Z around 1. The scattering length densities for acrylamide, sodium acrylate and DTAB are 1.56, 1.61 and $-0.25 \times 10^{10}\,\mathrm{cm}^{-2}$, respectively, and thus in D_2O ($\rho_S = 6.39 \times 10^{10}\,\mathrm{cm}^{-2}$) all three components are contributing to the total scattering cross-section. On D22, the data collected at 2 m and 14 m cover a range in wave vector: 1.5×10^{-3} Å^{-1} and 0.25 Å^{-1}, with an incident wavelength of 12 Å. They are treated according to the standard ILL procedures.

Figure 1 shows the autocorrelation function $g^{(2)}(t)$ for the scattered intensity measured on a PANa-PAM/DTAB solution at $c = 0.1\%$ and $Z = 1$. The relaxation functions labeled A, B and C in fig. 1 were recorded at scattering wave vectors $q = 1.6$, 2.1 and 3.0×10^{-3} Å^{-1}, respectively. Continuous lines through the data points are best-fit calculations using a single exponential decay, with an average decay rate 2Γ. In the inset, the linear dependence of $\Gamma(q^2)$ evidences the diffusive character of the concentration fluctuations. The diffusion coefficient is found at $D(c \to 0) = 6.7 \times 10^{-12}\,\mathrm{cm}^{-2}\mathrm{s}^{-1}$, corresponding to a hydrodynamic radius of $R_H = 370 \pm 10$ Å. The analysis of the autocorrelation functions in terms of cumulants reveals a relatively narrow polydispersity of the particle sizes. It is crucial to note that the results of fig. 1 are representative for a broad range of dilute solutions, those with $Z_C < Z < 100$. We have checked in addition that for dilute solutions, the zero wave vector intensity increases linearly with the concentration c (at fixed Z), a further indication of the formation of finite-size colloids.

Figure 2 compares the neutron scattering intensity received from three solutions at $c = 1\%$: pure surfactant ($Z = \infty$), pure polymer ($Z = 0$) and the intermediate solution PANa-

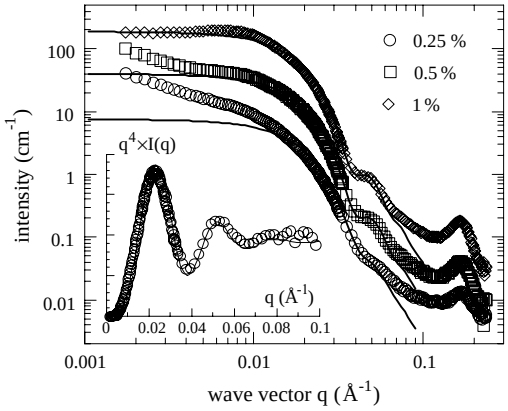

Fig. 3

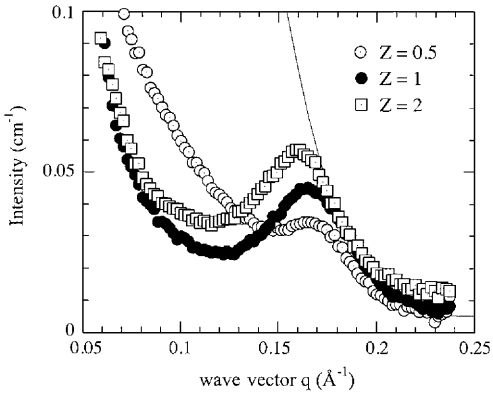

Fig. 4

Fig. 3 – Neutron scattering intensities measured on PANa-PAM/DTAB aqueous solutions at $c = 0.25\%$, 0.5% and 1% ($Z = 1$). The continuous lines are the contributions of the core of the aggregates ($R_C \sim 120\,\text{Å}$) and account for the scattering in the intermediate q-range. Inset: Porod representation of the intensity obtained at $c = 1\%$ and $Z = 1$. The continuous line corresponds to an adjustment using a polydisperse population of spherical and homogeneous particles with average radius $R_C = 124\,\text{Å}$.

Fig. 4 – Scattering maxima observed at large wave vectors in PANa-PAM/DTAB solutions at $c = 1\%$ and $Z = 0.5$, 1 and 2. The value of $q_0 = 0.16\,\text{Å}^{-1}$ corresponds to an average distance of 40 Å. The continuous line is the form factor of the DTAB micelles, as determined from the $c = 1\%$ solution.

PAM/DTAB at $Z = 1$. From the DTAB data ($Z = \infty$), one recognizes a broad correlation bump centered around $0.05\,\text{Å}^{-1}$ and originating from interactions between the electrostatically charged DTAB micelles [11]. The continuous line in fig. 2 is calculated using a form factor of polydisperse and homogeneous spheres of average radius $\bar{R} = 20.7\,\text{Å}$ (standard deviation, $(R^2 - \bar{R}^2)^{1/2} = 2.6\,\text{Å}$). This value of R as well as the aggregation number of 75 molecules per micelle that is derived from R are in agreement with those reported in the literature for DTAB micelles [12]. In fig. 2, deviations at low q are due to the intermicellar interactions, not taken into account in this simple analysis. The PANa-PAM/DTAB solution at $c = 1\%$ and $Z = 1$ exhibits three noticeable features. An intense forward scattering, a strong decrease of the intensity below $0.01\,\text{Å}^{-1}$ followed by an oscillation, and finally, at $q_0 = 0.16\,\text{Å}^{-1}$, a structure peak shown by an arrow. Note that, beyond the maximum of this structure peak, the intensity coincides with the form factor of DTAB micelles. In the following, these three q-regimes are discussed separately.

Intermediate q-range ($0.01\,\text{Å}^{-1} < q < 0.1\,\text{Å}^{-1}$). The data for the mixed system at $c = 1\%$ and $Z = 1$ are displayed in the inset of fig. 3 using here a Porod representation, which consists in plotting the product $q^4 \times I(q)$ *vs.* q. The oscillations observed in the Porod plot are characteristic of a spherical morphology and their damping, an indication of the polydispersity of the particles. Since the oscillations appear almost one decade in wave vector below that of pure DTAB (for which the first minimum is at $0.23\,\text{Å}^{-1}$), they are not arising from single surfactant micelles. The continuous line through the data corresponds to an adjustment using a polydisperse population of spherical and homogeneous particles, with average radius $R_C = 124 \pm 2\,\text{Å}$ and standard deviation 16 Å. The value of this radius is 1/3 that of the hydrodynamic radius revealed by light scattering. We therefore assign the scattering in the

intermediate q-range as arising from the core of the aggregates seen by light scattering. The observation of the Porod law indicates moreover that there exists an abrupt interface in terms of scattering length density between the core and the corona.

Low q-range ($q < 0.01\,\text{Å}^{-1}$). At the concentration of $c = 1\%$, the low q-scattering displays a very weak and broad structure factor (maximum at $6.6 \times 10^{-3}\,\text{Å}^{-1}$), which attests of interaction between the colloids. In order to get rid of these interactions, we have prepared solutions at 0.5% and 0.25% ($Z = 1$), using the technique described in the experimental section. The scattered intensity for these two solutions are shown in fig. 3. The overall shape of the scattering resembles strongly that at $c = 1\%$ (also included in fig. 3), except at low wave vector. Instead of a broad correlation maximum, we now observe at 0.25% and 0.5% that the intensity grows further with decreasing q. The continuous lines in fig. 3 are the contributions of the cores considered as homogeneous spheres, as derived from the Porod approach. For $c = 0.25$ and 0.5%, one gets $R_{\text{C}} = 120\,\text{Å}$. At low wave vectors, the deviations between the core contributions and the experimental data are interpreted as the signature of a corona. In this particular case, the corona is made of the poly(acrylamide) blocks.

We have tried to fit the intensities of fig. 3 using the core-shell form factor similar to those proposed recently by several authors [13]. The model assumes a homogeneous spherical core, and a corona characterized by a monomer density profile $n(r)$ varying as a function of the radial distance from the center of the colloid, as $n(r) \sim 1/r^{\alpha}$, where α can take values between 0 and 2. For instance, $\alpha = 4/3$ describes star-like profiles [14] and $\alpha = 2$ chains that are fully stretched [13]. Form factors using density profiles with $\alpha \sim 1.5$ have been computed and were found to describe the experimental scattering only qualitatively. For instance, we are able to show that for radii $R_{\text{C}} = 120\,\text{Å}$ and $R_{\text{H}} = 400\,\text{Å}$ (and assuming that the hydrodynamic radius is close to the actual radius of the micelles [15]), the model predicts an increase of the scattering at very low wave vectors, below $0.01\,\text{Å}^{-1}$. This is in agreement with the data of fig. 3. Quantitatively however, we are not able to account for the neutron intensity, at least for two different reasons. First, even at the lowest concentration investigated ($c = 0.25\%$), the structure factor might still be present and modify the contribution of the corona to the scattering at low q. Second, the inner structure of the core is complex and cannot be considered homogeneous as in the previous models (see below).

High q-range ($q > 0.1\,\text{Å}^{-1}$). At large wave vectors, the scattering is dominated by a peak at $q_0 = 0.16\,\text{Å}^{-1}$. The position of this peak, corresponding to a characteristic distance of 40 Å is found to be independent of the concentration (fig. 3). In fig. 4, the scattering intensities at $Z = 0.5$, 1 and 2 ($c = 1\%$) are shown in linear scales in order to emphasize that its position is also nearly independent of the surfactant-to-monomer ratio Z. It has been checked with X-rays (which has a much better resolution than SANS, $\Delta q/q \sim 3\%$ instead of 10%), that the bump is actually broad and does not result from the broadening of one or several Bragg reflections. For the structure peak at q_0, we have three independent indications that it is related to the surfactants. First, the location of the peak is found to shift to lower wave vector when the length of the amphiphile molecule is increased from 12 (as in DTAB) to 16 carbon atoms (as in cetyltrimethylammonium bromide). Second, the peak vanishes almost completely when the aliphatic chain of the surfactant molecule is deuterated, the solvent being still D_2O. Finally, the maximum at q_0 falls in the wave vector range where a scattering band is found in homopolyelectrolyte/surfactant precipitates [2–7]. For poly(sodium acrylate) with C12-surfactants, X-rays reveal a $Pm3n$ cubic structure recognized by several Bragg peaks in the range 0.1–0.2 Å^{-1}. We then conclude that DTAB spherical micelles are present in the core of the colloid. We assume, as for the polyelectrolyte/surfactant complexes [3,9], that they are linked together by the acrylate chains, and that the characteristic distance of $2\pi/q_0 \sim 40\,\text{Å}$ is

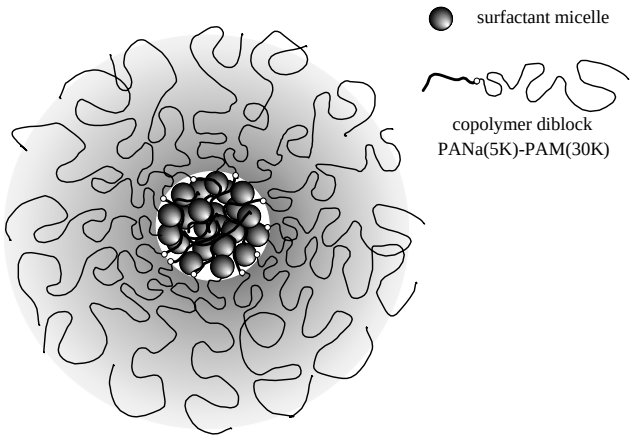

Fig. 5 – Schematical representation of a colloid formed by the association of neutral/polyelectrolyte diblocks and oppositely charged surfactants.

the intermicellar distance. In terms of symmetry, the core of the colloids can be considered as disordered. We finally derive the aggregation number for these mixed colloids. Using neutron scattering, we have investigated pure DTAB solutions as a function of the micellar volume fraction ϕ (between 0.01 and 0.5), and typically above $\phi = 0.01$, all spectra are showing a structure factor peak at wave vector, $q_{\mathrm{Max}}(\phi) = 0.185\phi^{1/3}$ where q_{Max} is expressed in $\mathrm{Å}^{-1}$. If we assume that this scaling is valid for the DTAB micelles inside the core of the colloid, the value of q_0 corresponds to a micellar volume fraction $\phi \sim 65\%$. Although estimated, this relatively high volume fraction is in agreement with the finding of an intermicellar distance of the order of twice the radius of a surfactant micelle. If we suppose in addition that there is an equal number of micelles and diblocks per colloid (since $Z = 1$), one obtains an aggregation number defined as the number of copolymers per agggregate of 120 ± 20. A schematical representation of the colloid formed by the association of neutral/polyelectrolyte diblocks and surfactant is proposed in fig. 5.

In conclusion, we have shown that neutral/polyelectrolyte diblock copolymer and oppositeley charged surfactants associate into colloidal aggregates which have an original core-shell microstructure. The originality resides in the core, which is described as a concentrated cluster of surfactant micelles, linked together by the polyelectrolyte blocks. We suggest that the mechanism of formation of these particles is identical to that of the phase transition encountered in the homopolyelectrolyte/surfactant mixtures. However, here the transition is arrested at a certain stage by the presence of the neutral block, preventing the macroscopic phase separation from occurring.

* * *

Fruitful discussions with M. JOANICOT, E. KALER and F. MOLINO are acknowledged.

REFERENCES

[1] KWAK J. C. T. (Editor), *Polymer-Surfactant Systems, Surfactant Science Series*, Vol. **77** (Marcel Dekker, New York) 1998.

[2] ANTONIETTI M., CONRAD J. and THÜNEMANN A., *Macromolecules*, **27** (1994) 6007; ANTONIETTI M. and CONRAD J., *Angew. Chem. Int. Ed.*, **33** (1994) 1869.

[3] Ilekti P., Piculell L., Tournilhac F. and Cabanne B., *J. Phys. Chem. B*, **102** (1998) 344; Ilekti P., Martin T., Cabanne B. and Piculell L., *J. Phys. Chem. B*, **103** (1999) 9831.
[4] Sokolov E., Yeh F., Khokhlov A., Grinberg V. Y. and Chu B., *J. Phys. Chem.*, **102** (1998) 7091; Zhou S., Burger B., Yeh F. and Chu B., *Macromolecules*, **31** (1998) 8157; Zhou S., Hu H., Burger B. and Chu B., *Macromolecules*, **34** (2001) 1772.
[5] Claesson P. M., Bergström M., Dedinaite A., Kjellin M., Legrand J.-F. and Grillo I., *J. Phys. Chem.*, **104** (2000) 11689.
[6] Ashbaugh H. S. and Lindman B., *Macromolecules*, **34** (2001) 1522.
[7] Kogej K., Evmenenko G., Theunissen E., Berghmans H. and Reynaers H., *Langmuir*, **17** (2001) 3175.
[8] Hansson P., *Langmuir*, **17** (2001) 4167.
[9] Bronich T. K., Kabanov A. V., Kabanov V. A., Yu K. and Eisenberg A., *Macromolecules*, **30** (1997) 3519; Kabanov A. V., Bronich T. K., Kabanov V. A., Yu K. and Eisenberg A., *J. Am. Chem. Soc.*, **120** (1998) 9941; Bronich T. K., Popov A. M., Eisenberg A., Kabanov V. A. and Kabanov A. V., *Langmuir*, **16** (2000) 481.
[10] Corpart *et al.*, US Patent N°6153705, Nov. 28, 2000; Taton D., Wilczewska A.-Z. and Destarac M., *Macromol. Rapid Commun.*, **18** (2001).
[11] Cabanne B., Duplessix R. and Zemb T., *J. Phys. (Paris)*, **46** (1985) 2161.
[12] Malliaris A., Le Moigne J., Sturm J. and Zana R., *J. Phys. Chem.*, **89** (1985) 2709.
[13] Willner L., Poppe A., Allgaier J., Monkenbusch M., Linnder P. and Richter D., *Europhys. Lett.*, **51** (2000) 628; Groenenwegen W., Egelhaaf S. U., Lapp A. and van der Maarel J. R. C., *Macromolecules*, **33** (2000) 3283; Won Y.-Y., Davis H. T., Bates F. S., Agamalian M. and Wignall G. D., *J. Phys. Chem.*, **104** (2000) 71.4.
[14] Daoud M. and Cotton J.-P., *J. Phys. (Paris)*, **43** (1982) 531.
[15] Pham Q. T., Russel W. B., Thibeault J. C. and Lau W., *Macromolecules*, **32** (1999) 2996.